Field modulated wavelength converters

Jonathon S. Barton, Matthew N. Sysak, Anna Tauke-Pedretti, Matthew Dummer, James Raring, Leif A. Johansson, Milan L. Mašanović, Daniel J. Blumenthal, Larry A. Coldren

Materials and Electrical and Computer Engineering Depts., University of California, Santa Barbara, 93106
jsbarton@engineering.ucsb.edu

ABSTRACT

We demonstrate 10Gbit/s operation of two different types of monolithic photocurrent driven wavelength converters (PD-WC). These photonic integrated circuits use a Semiconductor Optical Amplifier (SOA)-PIN photodetector receiver to drive an Electro-absorption (EA), or Mach-Zehnder (MZ) modulator that is integrated with a SGDBR tunable laser. We demonstrate improvements in optical bandwidth, insertion losses, device gain, and modulation efficiency.

Keywords: Wavelength conversion, high-speed modulators, optically controlled gate, tunable laser, semiconductor optical amplifier, Electro-absorption modulator, Mach-Zehnder modulator.

I. INTRODUCTION

Networking and infrastructure providers see great value in continuing to pursue technology that can lower costs yet provide increased flexibility and manageability of network capacity. Next generation networks using wavelength division multiplexing will benefit from highly functional large-scale Photonic Integrated Circuits (PICs). These new wavelength transparent networks will require important functions such as wavelength provisioning, add-drop multiplexing and packet switching that will need fast and dynamic wavelength conversion to eliminate wavelength blocking and wavelength management issues for high traffic networks. Traditionally, wavelength conversion is performed using a wavelength interchanging cross connect (WIXC) with conventional transponders and optical/electrical/optical (OEO) conversion. This approach does allow for clock recovery and 3R regeneration of the signal at the node. Unfortunately, these OEO devices consume increasingly large amounts of power at high bit rates, have a large footprint, and due to the electronics involved, lack bit-rate transparency[1-3]. Dynamic widely-tunable solutions that can cut power consumption, size, weight and ultimately costs are seen as essential, in not only terrestrial networks but increasingly avionic and ship based communication systems.

A number of different wavelength converter approaches have been explored. Typical approaches use either semiconductor optical amplifiers (SOAs) or Electro-absorption (EA) modulators with cross-gain modulation (XGM)[4], Four-Wave Mixing (FWM)[5], Difference Frequency Generation(DFG)[6], Nonlinear Optical Loop Mirror (NOLM)[7], SAGNAC[8], Michelson interferometer[9], delayed interference[10], Photocurrent Assisted Wavelength (PAW) conversion [11], and cross-phase modulation in fiber[12] and All Optical SOA Indium Phosphide (InP) based Mach-Zehnder structures [13,14]. Arrays of devices have been demonstrated in both in-plane and vertically illuminated[15] configurations. Also, tunable laser integrated devices have been demonstrated such as a wavelength selectable laser with all-optical wavelength converter[16]. Additionally, All Optical Label Swapping (AOLS) has been demonstrated with 40 Gbit/s RZ packets and 10Gbit/s labels using a Sampled Grating Distributed Bragg Reflector (SGDBR) laser integrated differential driven active Mach-Zehnder all-optical wavelength converter[17]. Another approach takes advantage of gain suppression by direct injection into either Super Structure Grating Distributed Bragg Reflector (SSGDBR)[18] or Grating Coupled Sampled Reflector (GCSR)[19] lasers.

The key issues that impact the performance of the wavelength converter include: insertion losses/coupling losses, wavelength dependence of output power, extinction ratio, input and output optical, input power dynamic range, power dissipation particularly with arrays, optical filtering of the input wavelength, bandwidth limitations such as carrier

Optoelectronic Integrated Circuits VIII, edited by Louay A. Eldada, El-Hang Lee,
Proc. of SPIE Vol. 6124, 612417, (2006) · 0277-786X/06/$15 · doi: 10.1117/12.656011

lifetime, cascadability, and chirp. Effective design needs to attempt to achieve adequate performance of all these metrics simultaneously.

II. PHOTOCURRENT DRIVEN WAVELENGTH CONVERSION

In this paper we present our latest results from a class of widely-tunable photocurrent driven wavelength converters (PD-WC). These devices operate by the generation of photocurrent in a detector, which changes the electric field across the depletion region in a reverse biased modulator. With this approach, switching speeds are not limited by carrier modulation effects such as carrier lifetime, and there is the potential for very high modulation bandwidths without requiring optical filtering of the input signal at the output. Very high optical bandwidths have been demonstrated with a similar optical gating approach using an integrated traveling wave Electro-absorption modulator (EAM) and high-speed detector[20]. In this manuscript, we demonstrate some of the first tunable laser integrated photocurrent driven 10Gbit/s capable devices based on both EAM and MZM devices. The structures benefit from a simple process and chip-to-chip optical gain (10dB), as well as operate at high data rates (10Gbit/s) with high extinction ratios (>10dB). These integrated devices make use of an optically pre-amplified receiver to eliminate the need for electrical amplification in the device. Additionally, they have the potential of exhibiting less dissipated power than conventional SOA based all-optical WC devices. PD-WCs are also inherently filterless due to spatial separation of the input and output ridge. In practice, stray light often can be coupled at the output through the substrate of photonic integrated circuits. With proper design with separation and curving of the waveguides, we achieve very high suppression of the input signal at the output (>40dB).

Monolithically integrated widely-tunable 2.5Gbit/s wavelength conversion has been previously demonstrated using an offset-QW integration platform with the direct modulation of SGDBR[21] and Bipolar Cascade SGDBR (BC-SGDBR) lasers[22] as well as externally modulated EA[23] and MZ[24] modulators integrated with a SGDBR laser, Semiconductor Optical Amplifiers (SOA), and a photodetector. Recently, 10Gbit/s operation has been demonstrated using a hybrid traveling wave series push-pull (SPP) MZM and amplified photodetector [25]. In this work, we aim to demonstrate fully integrated functionality, as well as reduce the high input power requirements and provide device gain. By using a more optimized SOA receiver design, input power requirements have been reduced considerably – down to approximately -10dBm. Improvements have also been made by modifying the integration platform growth structure. In the next section we examine the epitaxial structure in more detail.

III. MATERIAL STRUCTURE

Monolithic wavelength converters have been fabricated using a number of different integration platforms such as offset QW, quantum well intermixing, and butt joint regrowth techniques. A detailed discussion of these techniques is outlined elsewhere[26]. This manuscript will show some our latest results using a dual QW epitaxial structure which provides higher efficiency, higher bandwidth modulators and detectors, and potentially lower device insertion losses, when compared with the traditional offset quantum well (OQW) approach. This is achieved without modifying the simple fabrication sequence associated with the OQW platform or adding any regrowth steps [26-27].

It is well known that by implementing QWs in a modulator structure, one can improve the efficiency of modulation at lower DC biases on the modulator. The challenge is to simultaneously achieve low propagation losses and wavelength independence. We can take advantage of this added performance by using a dual QW structure in which offset gain QWs are used in the SOA and gain section of a SGDBR tunable laser, and wide and shallow centered QWs are used for the modulation and tuning regions. This approach improves the modulation efficiency considerably without increasing the propagation losses, or excessively restricting the wide wavelength range.

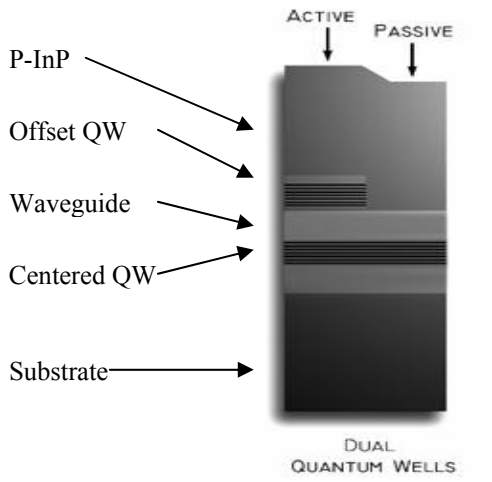

Layer	Doping	Thickness
P+InGaAs	1e19 cm^{-3} Zn	100nm
p- InP	1e18 cm^{-3} Zn	2µm
Offset QW	UID	106.5nm
Waveguide 1.3Q	5e16 cm^{-3} Zn	126nm
Centered MQW	UID	93nm
Waveguide 1.3Q	5e16 cm^{-3} Zn	126nm
InP Buffer	1e18 cm^{-3} Zn	1.8µm
N InGaAs	1e18 cm^{-3} Zn	100nm
InP buffer	1e18 cm^{-3} Zn	0.5µm
Substrate	Fe Semi-insulating	100µm

Fig.1 Dual Quantum Well growth structure

The base structure seen in fig. 1, is almost identical to the offset QW structure[24], except for a multi-quantum well region centered in the optical waveguide layer. The centered QW stack contains 7 x 9nm compressively strained (0.33 %) wells and 6 x 5nm tensile strained (0.075 %) barriers and has a photoluminescence peak at 1480 nm. With the proper design of the CQW stack, it is possible to achieve low propagation loss ($6cm^{-1}$), high injection efficiency (69%), high modulation efficiency and broad optical modulation bandwidths. Due to the reduced doping (5e16 cm^{-3} Si) in the waveguide region of the dual QW base structure, there is a significant bandwidth increase in comparison with OQW Franz Keldysh devices[26]. In addition, by utilizing shallow QW for the CQW stack, devices can operate under high waveguide optical power levels (>30 mW) without degradation of optical bandwidth. In the next two sections we will examine in more detail results from both fully integrated EAM and MZM based PD-WCs.

IV. ELECTROABSORPTION BASED DEVICES

Electro Absorption Modulator (EAM) based PD-WCs utilize two parallel waveguide ridges, one functioning as a receiver and the other functioning as a transmitter. The receiver consists of an SOA for amplification of the input signal and a photodiode for signal detection. The transmitter ridge consists of a widely-tunable SGDBR laser, output SOA and an EAM. The EAM and photodetector are interconnected such that the generated photocurrent in the detector drops across a termination load, resulting in a voltage swing across the EAM. For optimum performance, the SGDBR should provide wide tunability and high output power, the EAM should provide sufficient bandwidth for the desired data rate and high extinction efficiency, and the SOA/photodetector receiver needs to provide sufficient bandwidth and linear output power versus input power over the range required to drive the EAM. In other work, regrowth schemes are being explored for the separate optimization of the individual components[26]. Previously, 2.5Gbit/s operation had been demonstrated with an offset QW EAM based PD-WC[24], however more recent work using this very low capacitance dual QW structure enables 10Gbit/s non return to zero (NRZ) operation as illustrated in the next section.

1.1. Monolithic Dual QW EAM Based 10 Gb/s Wavelength Converter

In recent progress we have demonstrated the first 10Gbit/s NRZ monolithic widely-tunable EAM based PD-WC. Scanning electron micrographs showing the device layout are shown in fig. 2.

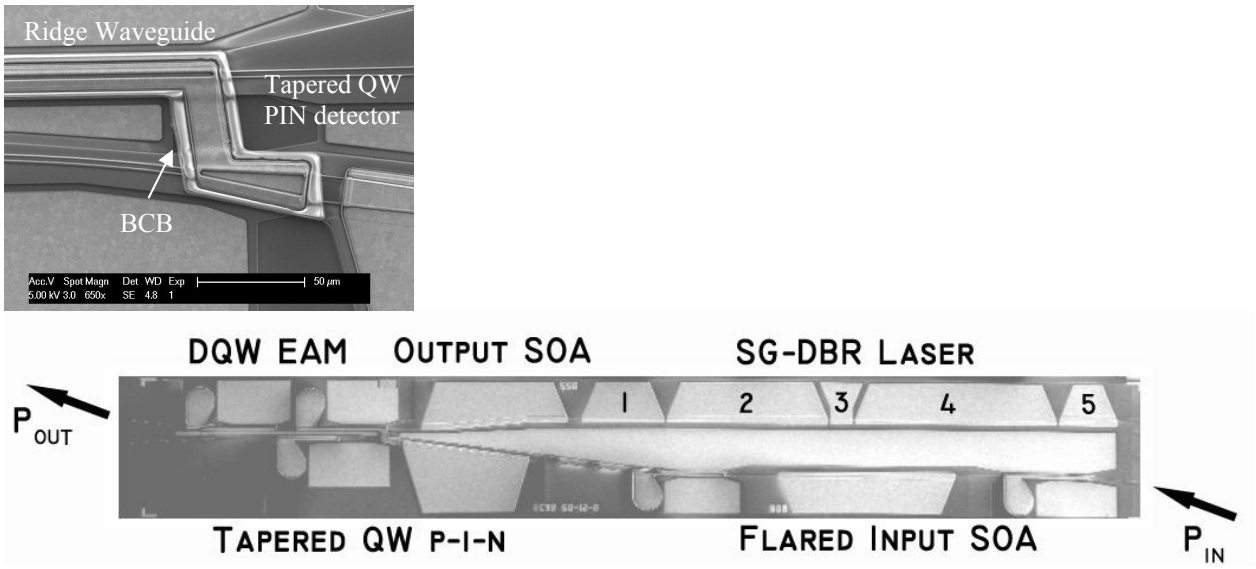

Fig. 2 Top view SEM of EAM based PD-WC device fabricated using the dual QW platform

For the EA modulator based devices, the input signal is fed into a passive curved waveguide as shown to the right of fig 2. It is amplified by two SOAs. The first SOA is 600 μm long and has a ridge width of 3.0 μm. The function of this SOA is to amplify the input signal from the fiber coupled level to just below the 1-dB gain compression for an optical amplifier of that particular ridge width. The second SOA is 400 μm long and has a flared waveguide ridge that is designed to maintain the overall photon density while the optical mode is expanded and the overall power level is increased. The second SOA is exponentially flared from 3.0 μm to 12 μm. The transmitter portion of the PD-WC is comprised of a four section SGDBR followed by a 550 μm long SOA for output amplification, and a shallow QW EAM electrode. The waveguide quantum well stack consists of seven 90 Å compressively strained wells and six 50 Å tensile strained barriers. The SEM inset in Fig. 2 shows the device electrode between the tapered QW detector and EAM ridge. Photo-bis-benzocyclobutene (BCB) low K dielectric is used under the high-speed modulator and detector electrodes to reduce the parasitic pad capacitances.. Additional optional passive section electrodes were integrated for power monitoring and diagnostics on both the input and output waveguides.

The SGDBR laser consists of a front mirror(1), gain(2), phase(3), rear mirror(4), and backside absorber(5), as depicted in fig. 2. Typical SGDBR wavelength spectra are shown for such a device in fig. 3a. The phase and mirror sections function to tune the wavelength of the laser over greater than 40 nm. The laser design is similar to that described previously[24]. Figure 3b shows the light/current/voltage characteristics for an untuned SGDBR laser with typical threshold currents close to 39mA.

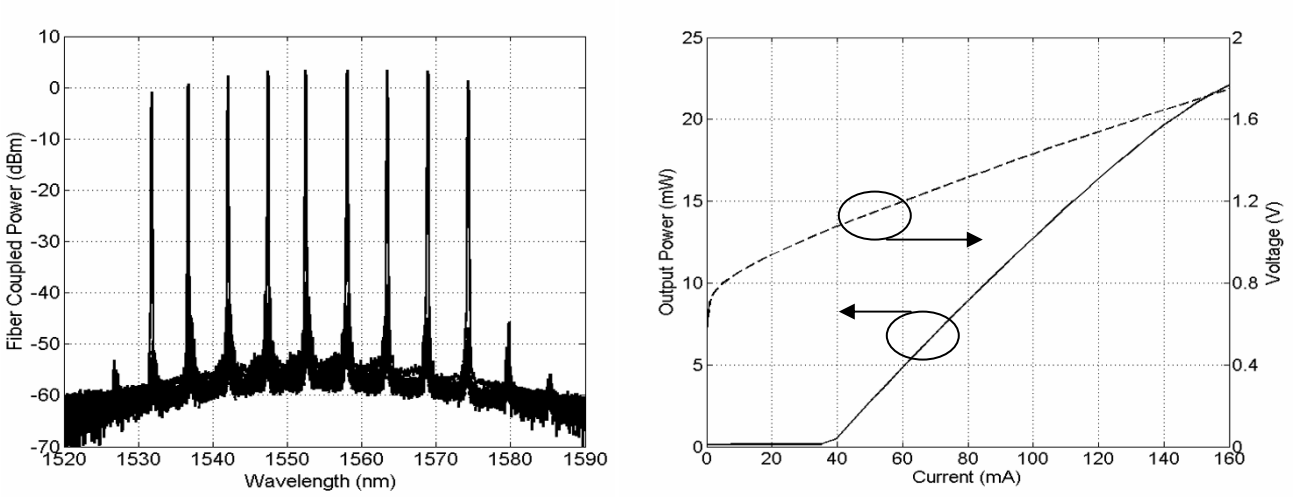

Fig. 3.(a) Tuning spectra and (b) light/voltage characteristics versus current for SGDBR fabricated on dual QW platform at 1555nm at 18 ^{0}C

One can see from fig. 4a that the wavelength shift possible under forward bias in the Sampled Grating (SG) Mirror sections using the dual QW structure is slightly improved with respect to a similar bulk waveguide SG mirror. With optimum MQW design, large refractive index changes are possible within the constraints of excessive optical losses[28]. As can be seen in Fig. 4b, the propagation losses through the device are increasingly wavelength dependent for long wavelength QW photoluminescence compositions. As mentioned before, the material used to fabricate the wavelength converter has a shallow QW PL peak centered at 1480nm. This corresponds to optical losses varying from approximately 15cm^{-1} at the lower limit of the C-Band to as low as 6cm^{-1} at 1565nm.

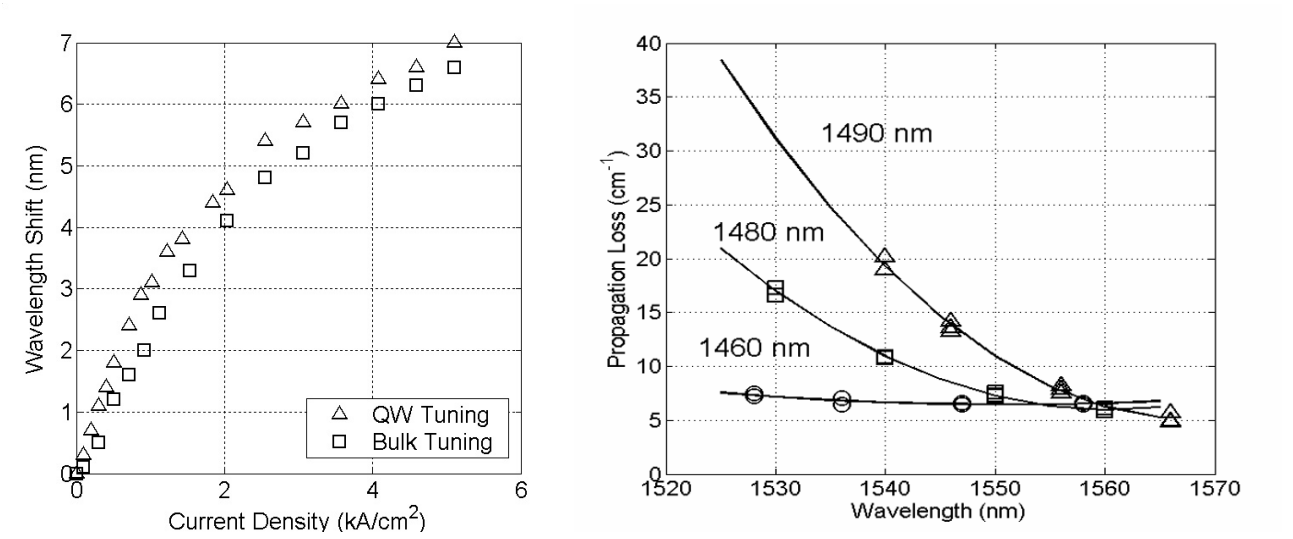

Fig. 4(a) Wavelength shift as a function of current density in the Sampled Grating mirror sections (b) Propagation loss versus operating wavelength for three different waveguide MQW designs employed in the dual QW platform[26]

Modulator efficiency is another important parameter that we wish to optimize. As can be seen in fig. 5a, the slope efficiency as a function of reverse bias can provide as high as two times the efficiency as a bulk InGaAsP Franz-Keldysh waveguide device based on the offset QW platform over the full wavelength range of operation. Since the efficiency improves with reverse bias, previous Franz-Keldysh based devices incurred large insertion losses in order to achieve sufficient extinction ratios and acceptable bit error rate (BER) performance. With the dual QW platform, much lower reverse biases can be used (2.5V-3.5V) for optimal efficiency which benefits from lower power dissipation and higher device gain due to the much lower insertion losses. As can be seen in fig. 5b, increased modulator length is advantageous for wavelength converter efficiency.

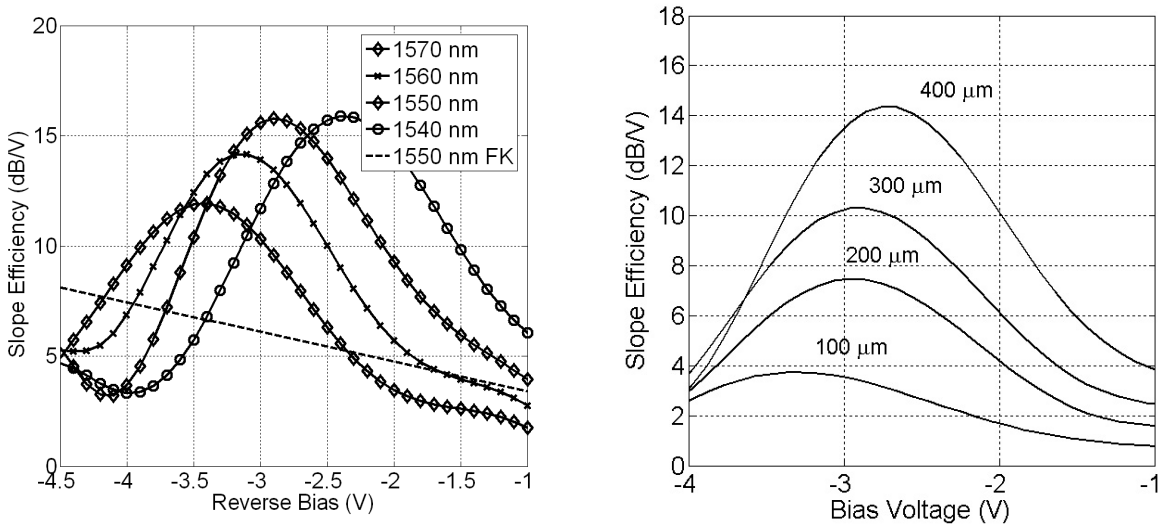

Fig. 5(a) Slope efficiency as a function of DC bias for different wavelengths using material with a shallow QW PL of 1480nm. Modulator is 400μm long. FK designates Franz-Keldysh offset QW structure (b) Slope efficiency as a function of DC bias for different electrode lengths at 1560nm

Key performance characteristics from wavelength converters with different EAM/detector schemes were measured to determine the optimum device layout for the EA based dual quantum well wavelength converters. The extinction ratio and output power versus reverse bias for wavelength converters comprised of a 50μm long tapered detector (as previously described) interconnected to a 200μm, 300μm, and 400μm long EAM are shown in fig. 6a and fig. 6b, respectively, at 10Gbit/s with a 50ohm termination. Wavelength conversion was performed between 1548 nm and 1550 nm and the input power level is –5 dBm. Input amplifier bias currents are set to maintain a current density of 6 kA/cm2 and the transmitter gain section is biased at 120 mA. The output transmitter SOA is biased at 75 mA.

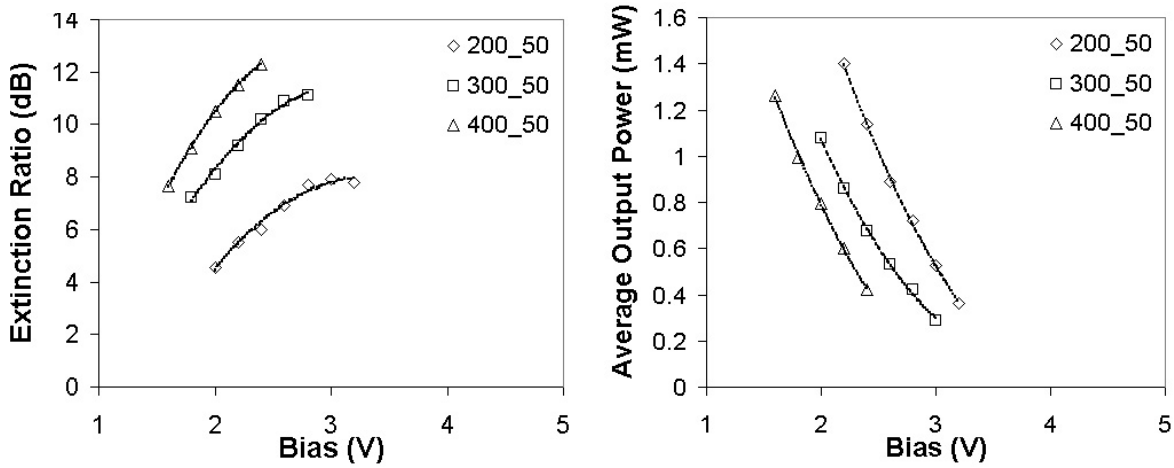

Fig. 6(a) Extinction Ratio (dB) vs. DC bias. (b) Average output power vs DC bias.
Wavelength converter 200μm long EAM- 50μm det / 300μm long EAM/50μm det / 400μm long EAM-50μm det. (centered and lined up?)

In Fig. 6, it can be seen that by increasing the length of the modulator, a higher extinction ratio and higher output power is possible with lower modulator bias.

The facet to facet device gain was measured for a device with a 300μm and 400μm long EAM electrode as can be seen

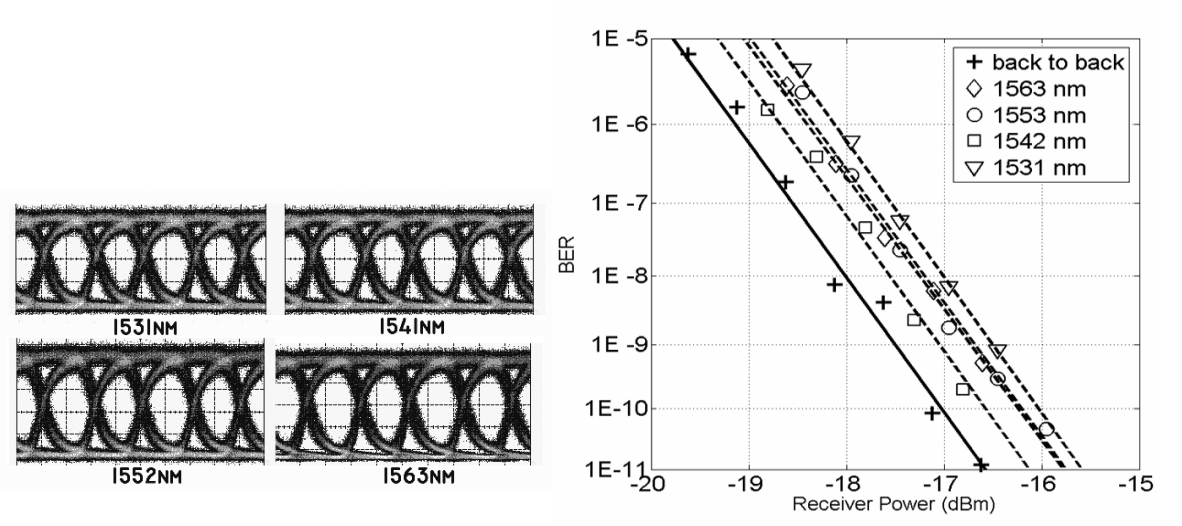

Fig. 8 (a) 10 Gb/s wavelength conversion eye diagrams for device with 400μm long EAM and 50μm long detector (b) BER measurements for received power for an input wavelength of 1548nm and various output wavelengths with a pattern length of 2^{31}-1

in fig. 8. 5-9dB of gain is demonstrated over the whole C-Band with an input power of -5dBm and over 10dB extinction ratio.

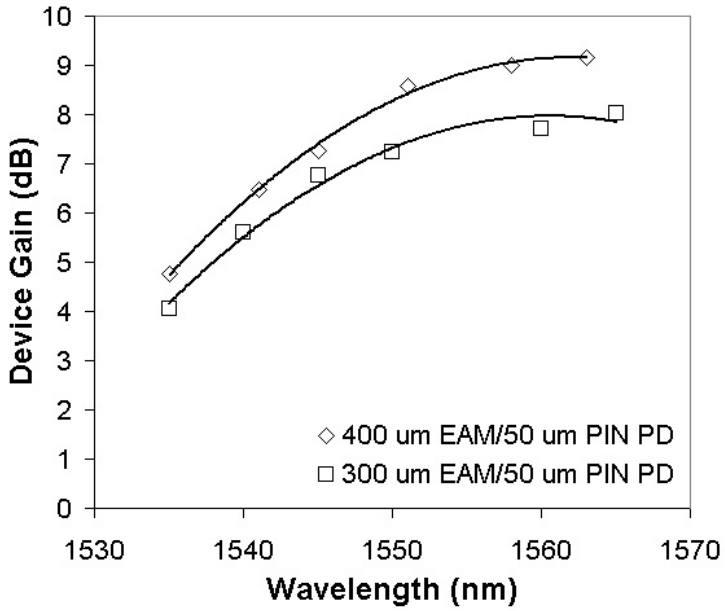

Fig. 8. Facet-to-facet device gain through device as a function of wavelength for input power of -5dBm. Coupling losses are 4.2dB for input and output lensed fiber.

Over the wavelength range, the SOA gain varies with a peak at 1550nm. Bias conditions were selected to achieve over 10dB extinction ratio at the output. As the 400μm long EAM based wavelength converter had sufficient optical bandwidth to operate at 10Gbit/s, it was chosen to perform bit error rate (BER) measurements. 10Gbit/s eye diagrams and BER measurements are given for an input wavelength of 1548nm to output wavelengths at 1531nm, 1541nm, 1552nm, and 1563nm using a pattern length of 2^{31}-1 Pseudo Random Bit Stream (PRBS). As can be seen in Fig. 7, all eye diagrams are open and clear. Greater than 10 dB of signal extinction was achieved at all wavelengths when biasing the EAM/photodetector in the 1.7-2.5V range. Less than 1-dB of power penalty can be seen over an operating

wavelength range of 32 nm. The reverse bias range and coupled-chip power used in this measurement was 1.7-2.5V and under -10 dBm, respectively. These results demonstrate the viability of single-chip wavelength conversion using the widely-tunable EAM PD-WC scheme.

VI. MACH-ZEHDNER BASED DEVICES

Two types of Mach-Zehnder based photocurrent-driven wavelength converters have been demonstrated recently using an OQW integration platform. The first configuration used photocurrent generated in a passive region photodiode to drive an integrated SOA-SGDBR transmitter with a single MZ lumped electrode[23]. Although appealing due to its polarization insensitivity, the device did not use any optical amplification leading to fairly high input power requirements. Without traveling wave electrodes, the optical bandwidth of the device is limited. More recently a hybrid integrated device using traveling wave series push pull (SPP) Mach-Zehnder modulator electrodes has demonstrated 10Gbit NRZ wavelength converter operation over a wide wavelength range with low power penalties[25]. This work used a SOA-PIN receiver to drive a 400μm long modulator[29]. A monolithic version of this device is shown in fig. 9. The total footprint of the chip is less than 1mm x 3.8mm. As this device is fabricated on a Fe-doped semi-insulating substrate, GeAuNiAu separate n-contacts are required in the laser, modulator, SOA and detector regions.

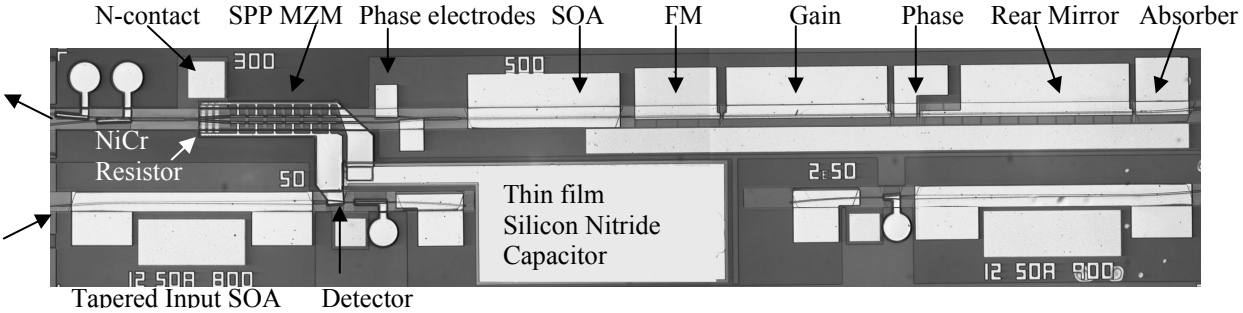

Fig. 9 Top view SEM of monolithic Series Push-Pull MZ based PD-WC device fabricated using the dual QW platform.

The input signal is fed into an 800 μm long tapered SOA from 3 μm to 9 μm which is detected in a 50 μm long shallow quantum well based tapered detector (from 9μm to 6μm). This photocurrent is used to drive a series push-pull (SPP) modulator on the transmitter side[30]. The device uses a SGDBR laser transmitter similar to as described earlier for the EAM based device followed by a 500 μm long SOA. The light is split into a Mach-Zehnder structure with 75 μm long phase electrodes on either branch to control the off state of the modulator. The series push-pull electrode structure uses eight T electrodes that are 50 μm long spaced by 10 μm for a total contact length of 400 μm long.

The electrical bias configuration is more complicated than that for the EAM case shown previously as shown in Fig. 10a. In the EAM case, there was a single DC bias on both the detector and modulator. This is ideal from a bias complexity perspective, however is not optimum from a bandwidth and insertion loss perspective. In the MZ case, we have integrated a thin film silicon nitride capacitor so that the detector can be biased relatively high (-4.5V) to maximize the bandwidth of the device, and a fairly low bias on the modulator electrodes (-1V) to achieve low insertion losses for the device and high efficiency. If both MZM electrodes are biased with the same value, one can also remove the DC component of the power dissipated across the integrated 50 ohm NiCr load resistor that is found at the end of the electrode. Each DC bias has a RF blocking inductor connection.

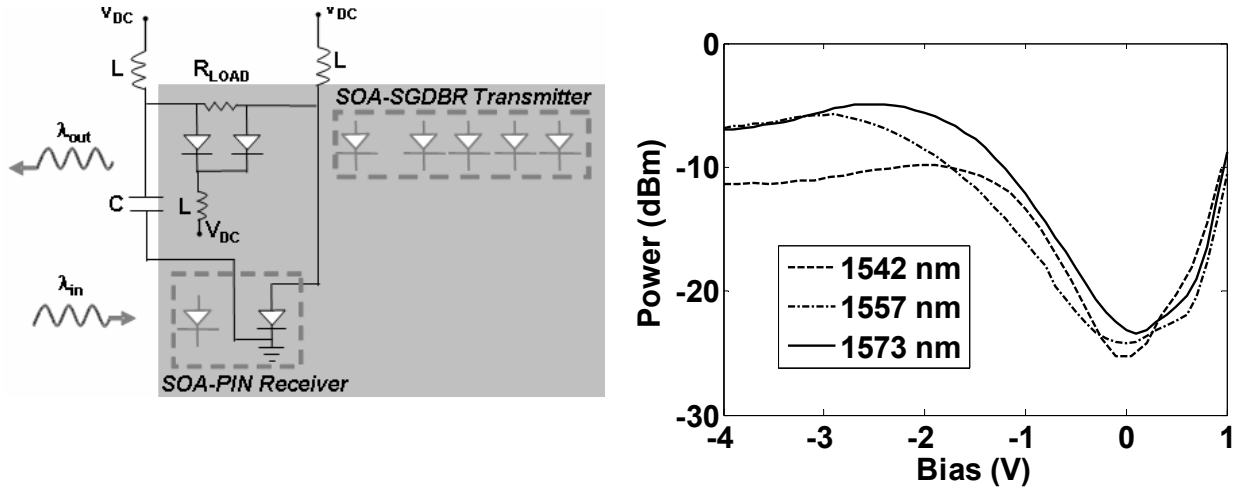

Fig. 10(a) Series Push-pull (SPP) MZ photocurrent-driven wavelength converter bias configuration (b) DC extinction curves for 300um long Dual QW MZ modulator as a function of wavelength.

Similar to the EAM case, the MZ device has high efficiency. DC extinction measurements are shown in fig. 10b for a transmitter with the following biases: I_{gain} = 100mA, I_{soa} = 100mA, P_{out} = 0.5mW.

Chirp is another important parameter for the wavelength converter. At high bit rates the dispersion in optical fibers will reduce the reach that is possible for a sub-optimal chirp parameter. A standard SOA based All-optical Mach-Zehnder interferometer uses mostly cross-phase modulation in one branch of the modulator to produce negative chirp in the non-inverting operation and positive chirp in the inverting operation. A tunable photocurrent-driven wavelength converter using a single-side drive Mach-Zehnder modulator will provide negative chirp with inverting operation and positive chirp with non-inverting operation[23]. The series push-pull configuration Mach-Zehnder modulator enables tailorable chirp, which can be achieved in both non-inverting and inverting operation. It is important to optimize the chirp parameter and extinction ratio simultaneously in order to maximize the transmission distance. Both branches of the Mach-Zehnder were biased to -1V with proper biasing of the phase electrode to achieve >10dB extinction ratio at the output. The power penalty was measured for 25km and 50km of Corning SMF-28 fiber using a 10Gbit/s 2^{31}-1 PRBS as can be seen in fig. 11.

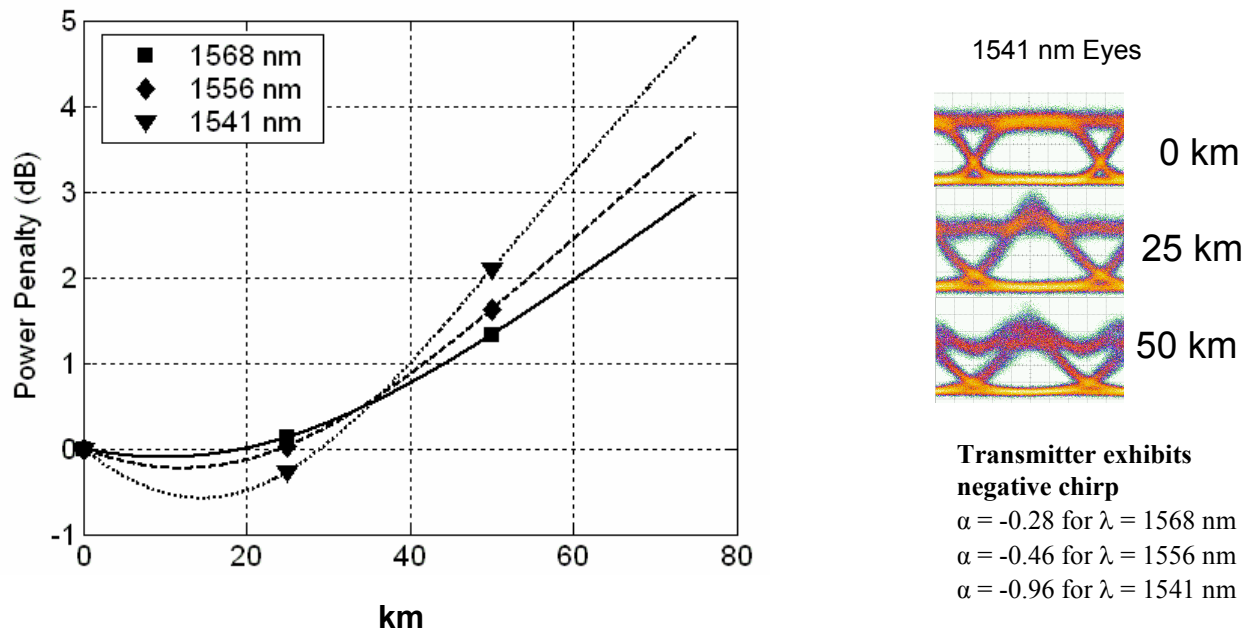

Fig. 11 Power penalty vs transmission distance for different output wavelengths biased with -1V on each MZ electrode. 1.87 Vpp input signal was applied to transmitter at different wavelengths for a 400μm long SPP MZM modulator.

Large signal chirp parameters were extracted for the different wavelengths as shown in Fig. 11.

VII. CONCLUSION

We have demonstrated high-speed wavelength conversion for two different photocurrent driven wavelength converter (PD-_WC) configurations. Both utilize a dual QW base structure that benefits from lower capacitance and improved efficiency. Both structures demonstrate the potential for wavelength conversion at 10Gbit/s with low power penalties(<2dB) over a wide wavelength range(30nm). With SOA design optimization, devices have been fabricated that have a net optical facet-to-facet gain (>5dB over whole wavelength range) and work well with very low input power requirements (<-10dBm).

PD-WC based on EAM technology have been fabricated and tested with both offset QW and dual QW integration platforms. With the introduction of the QW stack in the center of the waveguide, it has been shown that an improvement in the bandwidth efficiency product is possible for the EAMs while maintaining high injection efficiency and low propagation losses in the laser section. We have demonstrated wavelength conversion over 32 nm at 10 Gb/s with 10 dB optical extinction and less than 1dB power penalty with a PRBS of 2^{31}-1. Optimal wavelength conversion was obtained with -10dBm input power. This is a significant improvement over previously reported results for EA modulator based widely tunable wavelength converters.

The use of high-gain, high saturation power receivers coupled with high bandwidth efficient modulators have been shown to allow the realization of viable wavelength conversion at high bit rates. Series push-pull MZ PD-WCs have demonstrated error-free wavelength conversion over 37nm with <1dB power penalty, and low input power (1.3mW).

VIII. ACKNOWLEDGMENTS

This work was supported by Intel Corporation grant # TXA001630000, and DARPA MTO – CS-WDM grant #N66001-02-C-8026. We acknowledge Agility Communications for the regrowth of the MZM devices, and deposition of antireflection coatings.

IX. REFERENCES

1. Yoo S.J.B., "Wavelength Conversion Technologies for WDM Network Applications", IEEE J. Lightwave Technology, 14, 944-966 (1996).
2. Stubkjaer KE, Kloch A, Bukhave Hansen P, Poulsen HN, Wolfson D, Stockholm Jepsen K, Clausen AT, Limal E, Buxens A. "Wavelength converter technology." *IEICE Transactions on Electronics, vol.E82-C, no.2, Feb. 1999, pp.338-48. Publisher: Inst. Electron. Inf. & Commun. Eng, Japan.*
3. Yates Jennifer M., Michael P Rumsewicz, Jonathan P.R. Lacey, "Wavelength converters in dynamically reconfigurable WDM networks" IEEE Communications Surveys Second Quarter 1999.
4. Nesset D, Kelly T, Marcenac D. All-optical wavelength conversion using SOA nonlinearities. *IEEE Communications Magazine, vol.36, no.12, Dec. 1998, pp.56-61.*
5. Geraghty David F., Robert B. Lee, Marc Verdiell, Mehrdad Ziari, Atul Mathur, and Kerry J. Vahala,"Wavelength Conversion for WDM Communication Systems Using Four-Wave Mixing in Semiconductor Optical Amplifiers", IEEE Journal of Selected Topics in Quantum Electronics, Vol. 3, No. 5, Oct. 1997
6. C. Q. Xu, H. Okayama, and M. Kawahara, "1.5 pin band efficient broadband wavelength conversion by difference frequency generation in a periodically domain-inverted LiNbOs channel waveguide," *Appl. Phy. Lett,* vol. 63, p. 3559, 1993.
7. Cao, X.D. Jiang, M. Dasika, P. Islam, M.N. Evans, A.F. Hawk, R.M. Nolan, D.A. Pastel, D.A. Weidman, D.L. Moodie, D.G., "All-optical 40 GHz demultiplexing in a NOLM with sub-pJ switching energy" 1997. CLEO '97., Vol. 11, pp. 446-447, 18-23 May 1997.
8. Suzuki Y, Ito T, Shibata Y. "Monolithically integrated wavelength converter: Sagnac interferometer integrated with parallel-amplifier structure (SIPAS) and its application." 2002 LEOS Summer Topical Meetings IEEE.2002, ppWB2-12.
9. Wolfson D, Fjelde T, Kloch A, Janz C, Poingt F, Pommereau F, Guillemot I, Gaborit F, Renaud M. Detailed experimental investigation of all-active dual-order mode Mach-Zehnder wavelength converter. Electronics Letters, vol.36, no.15, 20 July 2000, pp.1296-7.
10. Leuthold J., C.H. Joyner, B. Mikkelsen, G. Raybon, J.L.Pleumeekers, B.I. Miller, K. Dreyer and C.A. Burrus 100Gbit/s all-optical wavelength conversion with integrated SOA delayed-interference configuration, Elect. Letts. Vol. 33, pp. 2137 (1997).
11. Hsu-Feng Chou, Yi-Jen Chiu, Adrian Keating, John E. Bowers, and Daniel J. Blumenthal, "Photocurrent-Assisted Wavelength (PAW) Conversion With Electrical Monitoring Capability Using a Traveling-Wave Electroabsorption Modulator", IEEE. Photonics Technology Letters, Vol. 16, No. 2, February 2004.
12. Olsson B-E, Ohlen P, Rau L, Blumenthal DJ. A simple and robust 40-Gb/s wavelength converter using fiber cross-phase modulation and optical filtering. IEEE Photonics Technology Letters, vol.12, no.7, July 2000, pp.846-8.
13. Wolfson D, Hansen PB, Kloch A, Fjelde T, Janz C, Coquelin A, Guillemot I, Garorit F, Poingt F, Renaud M. All-optical 2R regeneration at 40 Gbit/s in an SOA-based Mach-Zehnder interferometer. *OFC/IOOC'99. Optical Fiber Communication Conference and the International Conference on Integrated Optics and Optical Fiber Communications (Cat. No.99CH36322). IEEE. Part Suppl., 1999, pp.PD36/1-3 Suppl.. Piscataway, NJ, USA.*
14. Spiekman LH, Koren U, Chien MD, Miller BI, Wiesenfeld JM, Perino JS. All-optical Mach-Zehnder wavelength converter with monolithically integrated DFB probe source. *IEEE Photonics Technology Letters, vol.9, no.10, Oct. 1997, pp.1349-51.*
15. Demir HV, Sabnis VA, Jun-Fei Zheng, Fidaner O, Harris JS Jr, Miller DAB. "Scalable wavelength-converting crossbar switches." *IEEE Photonics Technology Letters, vol.16, no.10, Oct. 2004, pp.2305-7. IEEE.*
16. Broeke RG, Smit MK. "A wavelength converter with integrated tunable laser." *Integrated Photonics Research (Trends in Optics and Photonics Series Vol.91). Optical Soc. of America. 2003, pp.15-17. Washington, DC.*

17. Lal V, Masanovic M, Wolfson D, Fish G, Coldren C, Blumenthal DJ. "Monolithic widely tunable optical packet forwarding chip in InP for all-optical label switching with 40 Gbps payloads and 10 Gbps labels." 31st European Conference on Optical Communication. IEE. Part vol.6, 2005, pp.25-6 vol.6.
18. Yasaka H, Sanjoh H, Ishii H, Yoshikuni Y, Oe K. Finely tunable wavelength conversion of high bit-rate signals by using a superstructure-grating distributed Bragg reflector laser. *Journal of Lightwave Technology, vol.15, no.2, Feb. 1997, pp.334-41. IEEE.*
19. Lavrova OA, Rau L, Blumenthal DJ. "10-Gb/s agile wavelength conversion with nanosecond tuning times using a multisection widely tunable laser." *Journal of Lightwave Technology, vol.20, no.4, April 2002, pp.712-17 .IEEE.*
20. Kodama S, Yoshimatsu T, Ito H. 320 Gbit/s error-free demultiplexing using ultrafast optical gate monolithically integrating a photodiode and electroabsorption modulator. Electronics Letters, vol.39, no.17, 21 Aug. 2003, pp.1269-70. IEE.
21. Hutchinson J.M., J. Zheng, J.S. Barton, J.A. Henness, M.L. Mašanovic, M.N. Sysak, L.A. Johansson, D.J. Blumenthal, L.A. Coldren, H.V.Demir, V.A. Sabnis, O. Fidaner, J.S. Harris, and D.A.B. Miller, "Indium Phosphide-Based Optoelectronic Wavelength Conversion for High-Speed Optical networks"
22. Klamkin J., L. A. Johansson, J. T. Getty, J. M. Hutchinson, E. J. Skogen and L. A. Coldren, "Photocurrent Driven Widely-Tunable Wavelength Converter based on a Directly Modulated Bipolar Cascade SGDBR Laser ", LEOS 2004.
23. Barton J.S., Masanovic ML, Sysak MN, Hutchinson JM, Skogen EJ, Blumenthal DJ, Coldren LA. 2.5-Gb/s error-free wavelength conversion using a monolithically integrated widely tunable SGDBR-SOA-MZ transmitter and integrated photodetector. *IEEE Photon Tech. Letts, vol.16, no.6, June 2004, pp1531-3.*
24. Sysak MN, Barton JS, Johansson LA, Raring JW, Skogen EJ, M. L. Mašanović, Blumenthal DJ, Coldren LA. "Single-chip wavelength conversion using a photocurrent-driven EAM integrated with a widely tunable sampled-grating DBR laser." *IEEE Photonics Technology Letters, vol.16, no.9, Sept. 2004, pp.2093-5.*
25. Barton, J.S., A. Tauke-Pedretti, M. Dummer, M.N. Sysak, M.L. Mašanović, J.W. Raring, E.J. Skogen, and L.A. Coldren, "10Gbit/s Wavelength Conversion Using a Widely-Tunable Series Push-Pull Photocurrent-Driven Transmitter," IEEE Photon. Technol. Lett., vol. 17, pp. 1902-1904, 2005.
26. James W. Raring, Matthew N. Sysak, Anna Tauke-Pedretti, Mathew Dummer, Erik J. Skogen, Jonathon S. Barton, S. P. DenBaars, and Larry A. Coldren, "Advanced Integration Schemes for High-Functionality/High-Performance Photonic Integrated Circuits" SPIE Photonics West, 2006.
27. Barton J.S., A. Tauke-Pedretti, M. Dummer, E. J. Skogen, J. Raring, M. N. Sysak, L. A. Johansson, M. L. Masanovic, L. A. Coldren, "Widely-tunable photocurrent-driven wavelength converters", 5729-23, SPIE Photonics West, 2005.
28. Bennett, B., R. Soref, and J. DelAlamo, "Carrier-induced change in refractive index of InP, GaAs, and InGaAsP," IEEE Journal of Quantum Electronics, vol.26, pp. 113-122, Jan 1990.
29. Tauke-Pedretti, Anna, M. M. Dummer, J. S. Barton, M.N. Sysak, J. Raring, and L.A.Coldren," Integrated Photoreceivers with High Saturation Power, High Gain and >20GHz Bandwidth", Submitted to Photonics Tech. Letts. Sept 2004.
30. Tauke-Pedretti, Matthew N. Sysak, Jonathon S. Barton, James W. Raring, Matthew Dummer and Larry A. Coldren, "Monolithic Dual-Quantum-Well 10Gb/s Mach-Zehnder Transmitter"LEOS 2005 conference proc..